

UC Davis

UC Davis Previously Published Works

Title

Field Aging and Binder Fatigue Performance of Intermediate Asphalt Concrete Layers Containing Reclaimed Asphalt Pavement

Permalink

<https://escholarship.org/uc/item/41p563sm>

Authors

Rahman, Mohammad A

Harvey, John T

Jiao, Liya

et al.

Publication Date

2024-04-20

DOI

10.1177/03611981241240756

Copyright Information

This work is made available under the terms of a Creative Commons Attribution-NoDerivatives License, available at <https://creativecommons.org/licenses/by-nd/4.0/>

Peer reviewed

Field Aging and Binder Fatigue Performance of Intermediate Asphalt Concrete Layers Containing Reclaimed Asphalt Pavement

Mohammad A. Rahman¹ , John T. Harvey¹ , Liya Jiao² ,
Raghubar Shrestha³, and David J. Jones¹ 

Transportation Research Record
1–16

© The Author(s) 2024



Article reuse guidelines:

sagepub.com/journals-permissions

DOI: 10.1177/03611981241240756

journals.sagepub.com/home/trr



Abstract

In this research, field slab samples were taken from an asphalt pavement in a hot climate with a design life of 40 years at 2, 4, and 7 years of pavement age to determine aging behavior with time at different depths. The asphalt binders were extracted and recovered to evaluate the aging and fatigue performance of the intermediate layer of the asphalt pavement. The chemical and rheological aging properties of the binders were evaluated using Fourier transform infrared spectroscopy and a dynamic shear rheometer, respectively. The pavement included 25 mm (1 in.) open-graded and 75 mm (2 in.) polymer-modified layers over three intermediate layer lifts. The intermediate layer aging is mostly governed by the connecting air voids and binder content of the asphalt mixes. The variation in aging deeper than 100 mm (4 in.) below the pavement surface was minor because of the absence of heat and access to air, with similar aging parameter values observed for different years of field sampling indicating little to no aging after construction. A good correlation (R^2 values of 0.79–0.92) was observed between the chemical property (carbonyl index) and rheological properties of the extracted binder for the dense-graded asphalt concrete layers between 25 and 100 mm depths. The fatigue performance of these extracted binders was evaluated by performing linear amplitude sweep tests. The results indicate that binder fatigue performance initially improved with moderate levels of aging but started to decline under extreme aging conditions.

Keywords

field aging, fatigue performance cracking, chemistry, recycled materials, rheological properties

In the past, most asphalt pavement was designed for a lifespan of 20 years or less (1). However, with the adaptation of the mechanical-empirical design method and a better understanding of how to design asphalt pavements with lives of 40 years and longer, there has been a shift toward designing pavements with longer lifespans and minimal maintenance requirements, known as long-life pavement (1–4). A structural layer approach for achieving these designs, called asphalt concrete (AC) long life, uses performance-related specifications and testing for each of three AC layers: the top layer, intermediate layer, and rich bottom layer. A rubberized open-graded layer with a less than 40-year design life is also often included for safety and to help act as a sacrificial layer for top-down cracking. Long-life designs can also be achieved

using only the surface and intermediate layers. Each layer of long-life pavement is designed differently based on its specific function, with the intermediate AC layer being intended to resist repeated traffic loadings or fatigue (3) and provide bending resistance through its high stiffness and provide resistance to rutting. Thicker layers with stiffer asphalt mixes are expected to resist higher traffic repetitions (5).

¹Department of Civil and Environmental Engineering, University of California Pavement Research Center, University of California, Davis, CA

²Atlas Technical Consultants, Sacramento, CA

³California Department of Transportation (Caltrans), Sacramento, CA

Corresponding Author:

Mohammad A. Rahman, mohrahan@ucdavis.edu

In the first long-life design project, a stiffer virgin binder was used in the thicker layers to reduce bending at the bottom of the asphalt section (4). In recent years, the use of reclaimed asphalt pavement (RAP) without changing the virgin binder grade has been recommended for thick AC layers (3). The use of RAP is expected to produce stiffer AC mixes and increase fatigue resistance for thicker pavements (6–10). The degree of compaction also plays a crucial role in ensuring the performance of long-life AC pavements. Typically a maximum of 6% construction air voids is permitted for the intermediate AC layers (3, 4). For the rich bottom, a much lower air voids content (3% maximum) is used to help resist flexural bending and fatigue (3, 4). The mixes are designed by the contractor to meet performance-related specifications based on performance-related tests for flexural stiffness, flexural fatigue, and rutting with only aggregate gradation volumetric constraints. The decrease in the constructed air void contents is expected to reduce the rate of aging for the AC layers. The addition of highly aged RAP material (up to 25% in previous projects, potentially more in the future) to stiffen the intermediate layer causes more complexity in the asphalt aging behavior (11). The aged RAP is expected to contain lesser amounts of aging-prone volatile materials because of previous oxidative aging (12, 13).

The aging of asphalt mixes is a complex phenomenon and is mainly governed by the aging of the asphalt binder. In the presence of heat and oxygen, asphalt binder is prone to change its chemical and rheological properties and gain stiffness (11). The kinetics of asphalt aging can be divided into two general steps at a constant temperature, namely nonlinear fast-rate and linear constant-rate (14–19). Prior research has mostly focused on the aging of AC surface layers. With the introduction of long-life pavement, it is becoming important to also evaluate the aging in the thick intermediate AC layers as these layers will be expected to be in the field for a longer duration (40 years or more) than the surface layer of traditional AC pavement. It is also important to understand the effect of aging on binder fatigue performance for the intermediate AC layer and all layers. Development of tests and test result interpretation to characterize the fatigue of aged binders is a current concern for the asphalt industry.

One of the test procedures to evaluate the fatigue of asphalt binder is the linear amplitude sweep (LAS) test outlined in AASHTO T391-20. However, researchers have reported difficulties in interpreting the results of this current binder fatigue test while considering the aging effect (20–23). Material ejection during testing of stiffer binders has been reported by García Mainieri et al. (21). The material ejection leads to voids in the test samples

and results in stresses based on invalid assumptions. The measured post-peak stress–strain should not be included in data interpretation for binders containing RAP (21). Therefore, it is important to understand the asphalt binder fatigue performance with aging and validate that understanding from laboratory testing with field data. Based on that goal, the objectives of this study were as follows:

- evaluate the variation of aging parameters with depth and time for the intermediate AC layers containing RAP on a long-life project in a hot environment, to provide a better understanding for other long-life projects;
- evaluate the effect of percent air voids and binder content on the field aging;
- evaluate the correlation between binder rheological and chemical aging parameters;
- evaluate and understand the effect of field aging on binder fatigue performance containing RAP;
- evaluate the effect of extreme laboratory aging on binder fatigue performance as measured using the LAS procedure.

Materials and Methods

Pavement Structure

In 2012, a long-life asphalt pavement was built north of the City of Red Bluff in Tehama County, California. This pavement was built to carry heavy truck traffic (0.8 million equivalent single axle loads [ESAL] per year in the design lane in 2023) moving on Interstate 5. The pavement comprises six AC layers, as shown in Figure 1 and described in Table 1. The typical thicknesses of all six AC layers are shown in Table 1. The top open-graded rubberized AC layer (L6) was intended to be replaced after 8–12 years, while the remaining layers (L1–L5) were intended to last throughout the pavement design life of 40 years (3). The long-life surface layer (L5, below the open-graded layer) of the pavement was composed of a polymer-modified (PM) base binder (PG 64-28PM), while the same base binder (PG 64-16) was used for both the rich bottom layer (L1) and all intermediate layers (L2–L4). A higher amount of RAP (25% by weight of total aggregate) was used for the intermediate AC layers following the thick-stiff fatigue life concept. A slightly higher asphalt binder content was used by the contractor in the rich bottom layer to achieve constructed air voids of less than 3%, intended to provide additional bending and fatigue resistance, as shown in Table 1. The rich bottom had 15% RAP content (3).

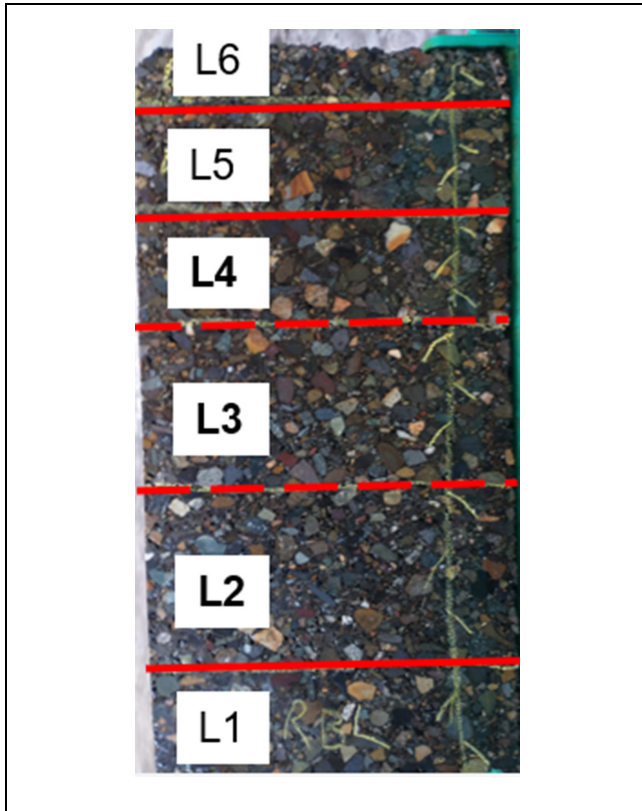


Figure 1. Slabs collected from the field.

The samples tested for this study were taken from slabs cut from between the wheel paths in the outside southbound lane of the project at different times after construction.

Pavement Climate Region

California experiences a wide range of climates, varying from hot desert areas with some of the hottest places in North America to coastal regions with milder

temperatures and cool summers (24). Based on the climate, California can be divided into nine different regions (24). The asphalt pavement considered in this study is located in the hot inland valley area (24). Figure 2 shows the variation in maximum daily air temperature from the National Climate Data Center (NCDC) for the representative weather station in the climate region (Fresno) from construction to sampling in different years. Figure 2 illustrates that the maximum daily air temperature was always greater than the freezing temperature of zero degrees Celsius. As shown in Figure 2, the highest value of maximum daily air temperature is 43.3°C for the asphalt pavement location considered in this study. The average annual maximum daily air temperature observed during this time period was 42.3°C.

Experimental Design

In this study, field slab samples from this long-life pavement were collected after 2, 4, and 7 years of pavement life within a 50 ft (15.24 m) pavement length to minimize the field variability of the samples in the longitudinal direction during construction. These slab samples were collected between the wheel paths of the truck lane. After each slab collection, the slab samples were stored in a 20°C (68°F) temperature-controlled room to minimize additional aging. Recovery of the extracted binder and binder testing were conducted by the same operator on the same equipment following the same procedures. The workflow diagram of this study is shown in Figure 3. The focus of this study is to evaluate the aging and fatigue performance of the intermediate AC layers (L2–L4). However, the surface L5 layer was also tested to evaluate the overall aging trend. The typical thickness of the L2 and L3 layers measured in the field was 3 in. (75 mm), while the L4 and L5 layers showed typical thicknesses of 2 in. (50 mm). These slabs were then subdivided to get a representative specimen at each 1-in. (25-mm) depth starting from the L2–L5 layers, as shown in Figure 4.

Table 1. Description of Long-Life Asphalt Concrete (AC) Layers Constructed at the Red Bluff

Layer ID	Layer name	Typical thickness	Base binder type	RAP content (%)	Binder content (% of total mass of mix (TMM) (based on binder extraction))
L6	Rubberized open-graded AC layer	1 in. (25 mm)	NA	NA	Not tested
L5	Polymer-modified surface AC layer	2 in. (50 mm)	PG 64-28PM	15	5.1–5.4
L2–L4	Intermediate AC layers	L2 and L3: 3 in. (75 mm) L4: 2 in. (50 mm)	PG 64-16	25	4.6–5.2 (Same base binder as L1)
L1	Rich bottom AC layer	2 in. (50 mm)	PG 64-16	15	5.7–5.8 (High)

Note: RAP = reclaimed asphalt pavement; NA = not available.

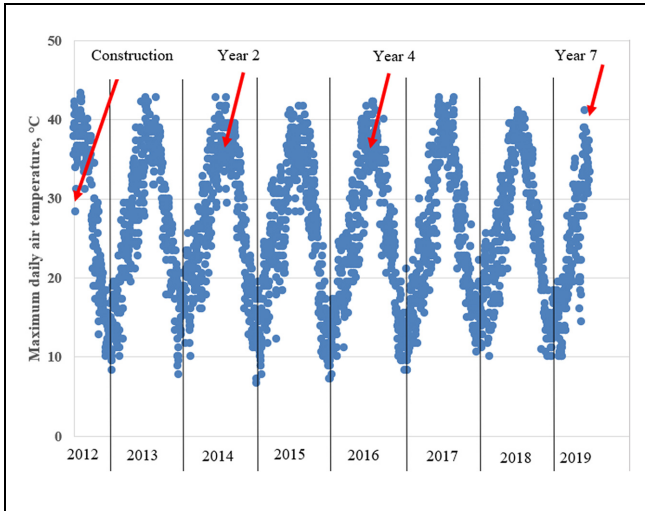


Figure 2. Variation in maximum daily air temperature from a nearby weather station from construction to sampling at different years, °C.

Therefore, three specimens were obtained from layers L2 and L3 and two specimens from layers L4 and L5. During the cutting process, approximately 0.2-in. (5 mm) of height was lost from each specimen. The final thickness obtained for each sub-lift specimen was approximately 0.8-in. (20 mm). Each sub-lift specimen was then marked based on the layer type and position of the sub-lift, as shown in Figure 4. For example, the bottom sub-lift of layer L2 was marked as “L2-1” (Figure 4).

Laboratory Testing

The bulk specific gravity of these slab specimens was determined in the laboratory following AASHTO T331. An auto-extractor was used to extract the asphalt binder

following ASTM D8159. The extracted binder was then recovered using the rotary evaporation process following ASTM D5404. The following binder tests were conducted in the laboratory to characterize the aging and fatigue performance of the asphalt binder.

Chemical Aging Test. The chemical properties of the extracted binders were evaluated using Fourier transform infrared spectroscopy (FTIR). The spectra measured by the FTIR were recorded in a reflective mode, from 4000 to 400 cm⁻¹, at a resolution of 4 cm⁻¹. For each measurement, an average value of 24 scans was recorded. Nine replicate measurements were taken to ensure that representative measurements were collected for each binder sample. The carbonyl area (CA) index determined from FTIR was used to track chemical properties with aging. The tangential integration of the CA index was calculated between the upper and lower wavenumbers (1671 and 1720 cm⁻¹) (25). The aliphatic band at 2923 cm⁻¹ was used to normalize the spectra and eliminate any variability introduced by the operator and any background impacts between repeat measurements. The previous literature suggested that this aliphatic band structure is not affected by aging over time (26, 27). The following equation was used to integrate the CA index:

$$I_i = \int_{w_{l,i}}^{w_{u,i}} a(w)dw - \frac{a(w_{u,i}) + a(w_{l,i})}{2} \times (w_{u,i} - w_{l,i}) \quad (1)$$

where I_i is the index of area i , $w_{l,i}$ is the lower wavelength integral limit of area i , $w_{u,i}$ is the upper wavelength integral limit of area i , and $a(w)$ is the absorbance as the function of wavelength.

Rheological Aging Test. Rheological properties were determined with a dynamic shear rheometer (DSR). The

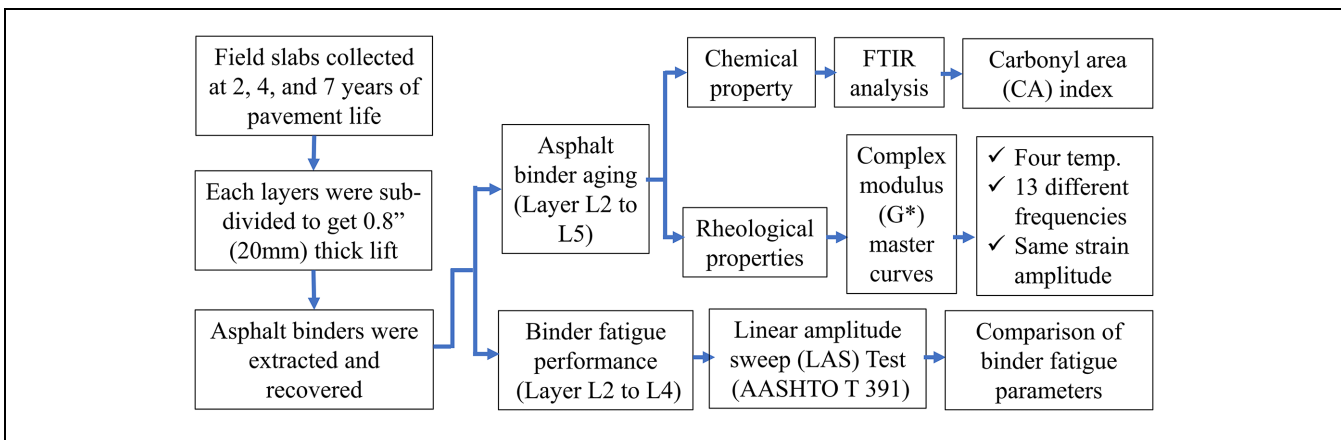


Figure 3. Workflow diagram of this study. Note: FTIR = Fourier transform infrared spectroscopy.

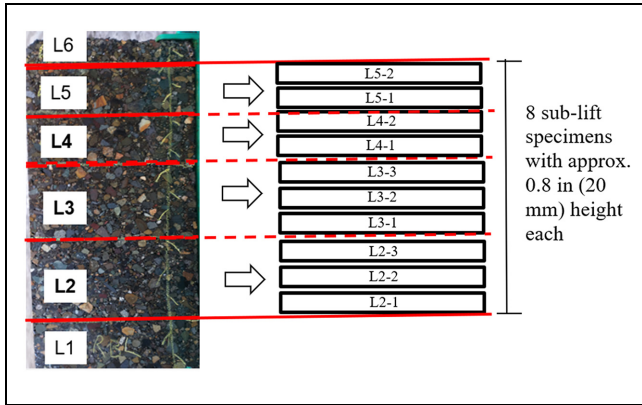


Figure 4. Schematic of the field slab specimens for binder extraction.

complex shear modulus (G^*) and phase angle (δ) values at four different temperatures (5°C , 10°C , 25°C , and 40°C) and at 16 different testing frequencies (0.02–15.92 Hz) for all extracted binders were evaluated. A symmetric sigmoidal fit function was used to convert the frequency sweep data into a master curve at the reference temperature using the fit function. The reference temperature considered in this study was 15°C . The following aging parameters calculated with the G^* and δ values were considered in the study.

1. Glover–Rowe (GR) parameter: the GR parameter was calculated using G^* and δ values at 15°C and 0.0008 Hz (0.005 rad/s), as shown in Equation 2. This parameter is expected to increase with an increase in aging level (28):

$$GR = \frac{G^* \cos^2 \delta}{\sin \delta} \quad (2)$$

2. The G^* value at 64°C and 10 Hz: the literature suggests that the binder's G^* value at 64°C and 10 Hz is appropriate for evaluating the aging of asphalt. Higher G^* values at 64°C and 10 Hz are associated with greater aging levels (13).
3. Crossover modulus (G_c^*): the crossover modulus is defined as the modulus when the phase angle (δ) is 45° . The G_c^* values decrease with an increase in binder aging (11, 29).
4. Crossover frequency (ω_C): the crossover frequency is defined as the frequency when the phase angle (δ) is 45° . The degree of aging decreases the ω_C values.

Binder Fatigue Test. In this study, the LAS test was performed according to the AASHTO T391-20 method for

all binders extracted from intermediate layers (L2–L4). This test was conducted at 25°C considering the typical intermediate temperature of the pavement located in Red Bluff. The LAS test was conducted using 8-mm parallel plate geometry with a 2-mm gap setting in the DSR. For each extracted binder type, a minimum of two replicates were tested. Firstly, frequency sweep tests were conducted at 0.1% strain level over a range of frequencies from 0.2 to 30 Hz. Then amplitude sweep tests were conducted at a constant frequency of 10 Hz at 31 different strain levels (from 0.1% to 30%) in the strain-control test mode. The analysis of LAS testing results was conducted following the AASHTO T391-20 method. In this method, the damage at failure is defined as the damage corresponding to a 35% reduction in the undamaged value of the loss modulus ($|G^*| \sin \delta$). The fatigue model parameters (A_{35} and B) were calculated accordingly. The following equation was used to calculate the fatigue life (N_f):

$$N_f = A_{35} (\gamma_{\max})^{-B} \quad (3)$$

where γ_{\max} is the maximum expected binder strain for a given pavement structure (%).

The values of γ_{\max} are expected to be about 7.8–510 times higher than the strain experienced by the AC mixture (30). A new parameter ($\Delta|G^*|_{\text{peak } \tau}$) proposed by García Mainieri et al. (21) was also used to evaluate the fatigue performance of the asphalt binder. The $\Delta|G^*|_{\text{peak } \tau}$ value represents the reduction in the complex modulus (G^*) from the start of the test until the peak shear-stress (τ) condition. A higher $\Delta|G^*|_{\text{peak } \tau}$ value indicates better fatigue resistance (21). According to García Mainieri et al. (21), the asphalt binder is expected to perform better with respect to fatigue when it tolerates greater loss in stiffness before the shear resistance decreases after reaching the peak.

Sensitivity Analysis

The effect of extensive laboratory aging on field sub-lifts was also evaluated in this study. This was undertaken to observe the changes in aging indices and binder fatigue parameters with extensive aging. The current laboratory long-term aging protocol is 5 days at 85°C for compacted AC mixes according to AASHTO R30-22. This procedure is expected to simulate 1–3 years of aging for a compacted dense-graded surface mix. In this study, the L3-2, L3-3, and L3-1 sub-lifts collected at year 4 were oven aged in the laboratory for 5, 13, and 20 days, respectively, at 85°C , as shown in Figure 5. The slabs were vertically placed with the maximum area exposed to oven heat to promote uniform aging conditions across the material during long-term laboratory aging. Then the aged sub-lift binders were extracted following the ASTM



Figure 5. Extensive laboratory aging for selected sub-lifts.

D8159 method and recovered using the rotary evaporation process following the ASTM D5404 method. This type of extensive aging may not occur in the field, especially for the intermediate AC layers. However, applying extensive aging in this study is important to evaluate the effect of aging on the binder's rheological and chemical parameters. This is expected to help one to understand the changes in binder fatigue performance under extreme aging conditions. There is a gap in the current literature concerning the effect of aging on binder fatigue performance.

Results and Discussion

Aging in the Intermediate AC Layers

Figure 6 presents the variations of the carbonyl area (CA) index, percent air voids, and percent binder contents by total weight of mix (TWM) with depth for different years of pavement sampling (2, 4, and 7 years). In the dense-graded layers near the surface of the pavement (beneath the open-graded layer), the aging was found to increase consistently with the increase in pavement sampling years. The CA indices observed at the top of layer L5 (L5-2) collected at years 2, 4, and 7 were 1.29, 1.51, and 1.88, respectively. A p -value of 1.49×10^{-6} was observed in a two-tailed t -test conducted for CA values of sub-lift L5-2 between years 2 and 7. This indicates a significant difference between the aging indices at a 95% confidence level. This is attributed to the effect of greater pavement temperature and access to air in the top surface layers (31, 32). The effect of greater pavement surface temperature and air access could be observed down to a depth of 4 in. (100 mm) below the top of the asphalt pavement (Figure 6). Below the depth of 4 in. (100 mm), similar CA indices were observed for all years of pavement sampling and it was also observed that they were generally similar at all depths below 4 in. The CA indices

observed at 4.5 in. (112.5 mm) (sub-lift L4-1) depth for 2, 4, and 7 years of pavement sampling were 0.77, 0.74, and 0.79, respectively. A p -value of 0.54 was observed in a two-tailed t -test conducted for CA values of sub-lift L4-1 between years 2 and 7. This indicates that differences between the aging indices are not significant at a 95% confidence level.

For intermediate AC layer L3, slightly lower CA indices were observed for slabs taken at year 7 compared to year 2. The CA indices observed for year 2 at the bottom (L3-1), middle (L3-2), and top (L3-3) of the L3 layer were 0.93, 0.93, and 0.94, respectively. After 7 years in the field, the CA indices found for L3-1, L3-2, and L3-3 sub-lifts were 0.76, 0.78, and 0.81, respectively. Reasons for slightly lower CA indices at year 7 could be the lesser impact of greater heat at intermediate layers and the higher degree of compaction achieved for slabs collected at year 7. This may also be attributed to the variability of RAP and slight differences in silo time during construction. Even though these slabs were taken within the same 50 ft (15.24 m) pavement length, there are still differences in the degree of compaction among different slab samples from the same depth at different years, as shown in Figure 6.

The relationship between compaction level and aging was also noticed at the bottom of the L2 layer (L2-1 sub-lift) for all years of pavement sampling. Relatively higher percent air voids were observed for the L2-1 sub-lift, resulting in higher CA indices. At year 4, the CA indices observed for the L2-1 and L2-2 sub-lifts were 1.21, and 0.89, respectively. The interface between two different AC layers (L1 and L2) might cause this poor compaction at the L2-1 sub-lift. In the field, the compaction roller was moved at the top of the L2 layer (L2-3 sub-lift), leaving insufficient compaction energy for the bottom of the L2 layer (L2-1 sub-lift). Therefore, better compaction was observed for the L2-3 sub-lift compared to the L2-1 sub-lift.

The percentage of air voids was considered in this study to evaluate the accessibility of oxygen. Typically, higher air voids and longer in-service years are expected to cause more aging. However, the permeability within sub-lifts might be a better indicator to evaluate the effect of access to oxygen on binder aging. For example, The CA indices observed for sub-lift L2-1 after 4 and 7 years in the field were 1.21 and 0.98, respectively. The air voids contents for sub-lift L2-1 at years 4 and 7 were 5.3% and 7.5%, respectively. The lower aging index for sub-lift L2-1 at year 7 compared to year 4 is likely attributable to the lower air voids in the sample taken in year 7, despite the three extra years in the field. Better compaction in the layers L3 and sub-lift L2-3 in the year 7 sample than the compaction in those same layers in the year 4 sample may have also been caused by less oxygen accessibility in

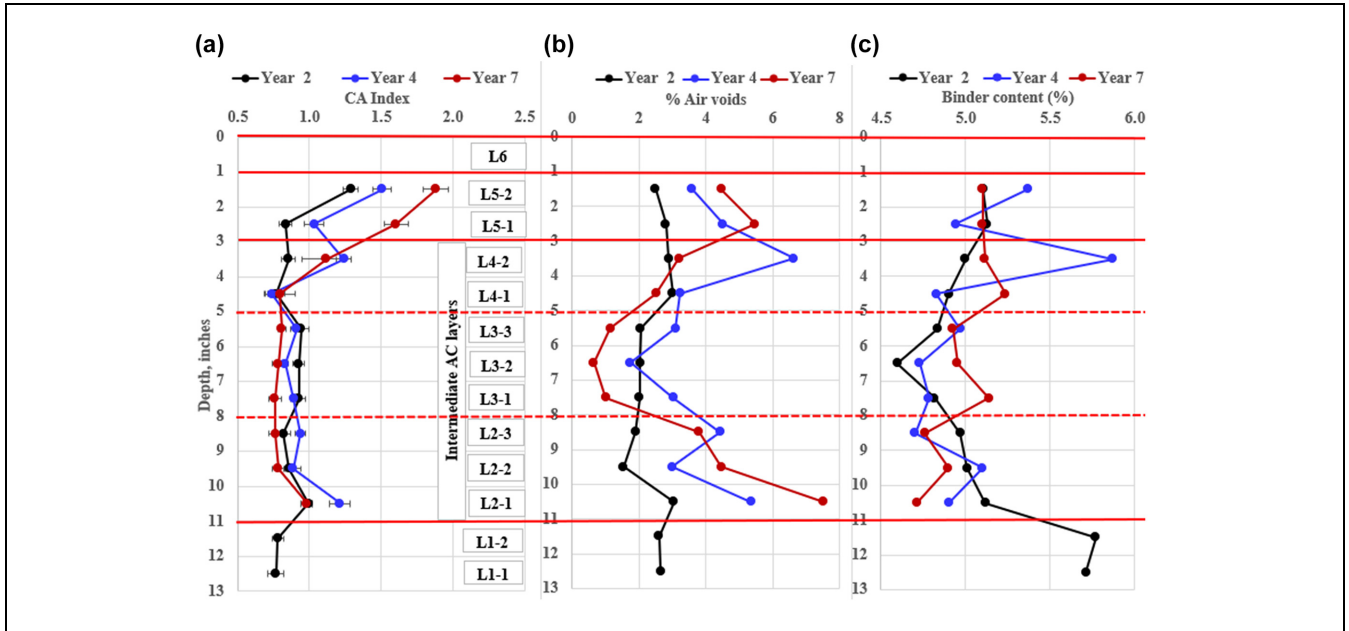


Figure 6. Variation of (a) carbonyl area (CA) index, (b) % air voids, and (c) % binder content with depth for different years at pavement sampling.

Note: AC = asphalt concrete. Error bars indicate one standard deviation of results.

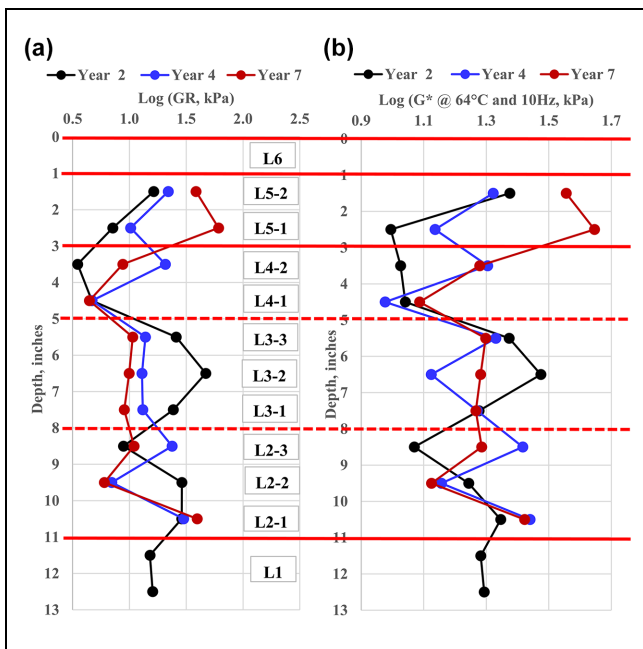


Figure 7. Variation of rheological parameters (a) log (Glover-Rowe [GR] parameter, kPa) and (b) log (G^* @ 64°C and 10Hz, kPa) with depth for different years at pavement sampling.

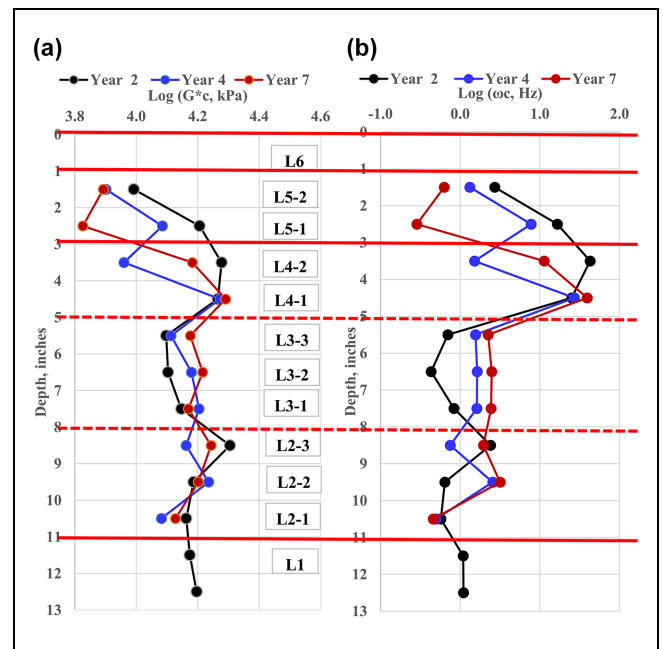


Figure 8. Variation of rheological parameters (a) log (G_c^* , kPa) and (b) log (ω_c) with depth for different years at pavement sampling.

the year 7 sub-lift L2-1 sample. It therefore appears that the connectivity of pores also plays an important role in controlling the aging of AC layers in the field. Finally, the binder content found for the slabs collected from the rich bottom layer (Layer L1) was higher (0.5%–0.7%

higher binder content by TWM) than that for the other layers, as expected from the mix design (Figure 6c).

Figures 7 and 8 illustrate the variations in rheological properties of extracted binders at different depths and different years of field sampling. The rheological

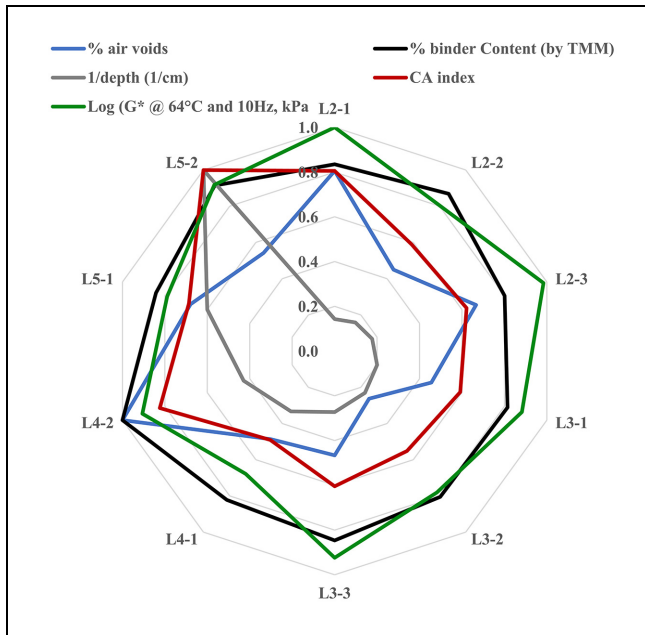


Figure 9. Radar plot showing different parameters (% air voids, % binder content, 1/depth, carbonyl area (CA) index, and log [G^* at 10 Hz and 64°C, kPa]) for sub-lifts collected at year 4.

Note: TMM represents the total mass of the asphalt concrete mix.

parameters of the binders followed a pattern similar to that of the chemical parameters. More aging was observed for year 7 slabs at the top of the AC layers. The GR parameter and complex modulus (G^*) exhibited an increase with aging, while the crossover modulus (G_c^*) and crossover frequency (ω_c) showed a decrease. The GR values observed for the top of the PM AC layer (L5-2) after years 2 and 7 in the field were 16 and 39 kPa, respectively. Similarly, the G^* at 64°C and 10 Hz increased from 24 to 36 kPa for years 2 to 7 for the L5-2 sub-lift. The G_c^* values were found to decrease from 9818 to 7813 kPa for the same sub-lift from 2 to 7 years. A decrease of 2.71 to 0.63 Hz in ω_c was observed for the same case. This is mainly attributed to the effect of greater heat on the top surface layers. Similar rheological aging parameters were observed at a depth of 4.5 in. (112.5 mm) for sub-lift L4-1, as shown in Figures 7 and 8. At a depth of 3.5 in. (L4-2), greater aging was observed for year 4 compared to year 7. As shown in Figure 6, the L4-2 sub-lift collected at year 4 has much higher air voids and binder contents compared to other years. Therefore, greater access to oxygen for that sub-lift likely caused more aging. Sub-lift L3-2 at year 2 was found to show higher rheological aging indices (GR, G^*) compared to other years. However, a slightly higher chemical index was observed for sub-lift L3-2 at year 2, as shown in Figure 6. Greater variations with depth were observed in GR and G^* values for layers L2 and L3 compared to the G_c^* and ω_c values (Figures 7 and 8).

Figure 9 shows the radar plot of change in aging indices (CA index and complex modulus) with percent air voids, percent binder content, and the inverse of depth (1/depth) for slab samples collected at year 4. The 1/depth was used to consider the change in aging with pavement depth. For better visualization, the values of each variable were normalized by the maximum observed value of the corresponding variable. For example, the maximum percent air voids value observed for samples collected in year 4 was 6.6%. All other percent air voids values were divided by 6.6 to better visualize the effect of percent air voids on aging indices. Figure 9 shows that both the CA index and binder complex modulus were found to show a similar trend. Sub-lift L4-2 shows slightly higher aging indices because of the higher percentage of air voids, as discussed earlier. Sub-lift L5-2 shows greater aging indices because of its nearness to the pavement surface (larger 1/depth value).

Binder Chemical to Rheological Properties

Figure 10 shows the correlations between the chemical parameter (CA index) and different rheological parameters. Previous studies suggest that the CA index is a more reliable chemical parameter in tracking the aging of extracted binders compared to the sulfoxide index (7, 11). Therefore, the CA index was considered in this study to track the aging of field slabs. Rahman et al. (11) suggested that the correlation between binder chemical and rheological properties depends on the base binder grades and sources. For mixes with RAP, the blended binder properties including the properties of the RAP also play an important role in defining the relation between chemical and rheological parameters (11). Therefore, the correlations are shown according to different field AC layers in Figure 10. Good correlations were observed between chemical and rheological properties for the L4 and L5 layers (R^2 values of 0.79–0.92), which have relatively large differences in aging and therefore in chemical and rheological properties. The scale for correlation assessment was 0–1 for all cases. However, poor to medium correlations (R^2 values of 0.25–0.70) were found for intermediate L2 and L3 layers below 4 in. (100 mm) depth, as expected because there is little variability of chemical or rheological properties at those depths. The lack of variability is because there is little or no aging as a result of the absence of ultraviolet (UV) ray penetration, a lower degree of heat exposure, and less accessibility of oxygen for the L2 and L3 layers.

Binder Fatigue Performance of Intermediate Layers

Figure 11 shows the change in shear stress with applied shear strain for different extracted binders. The binders

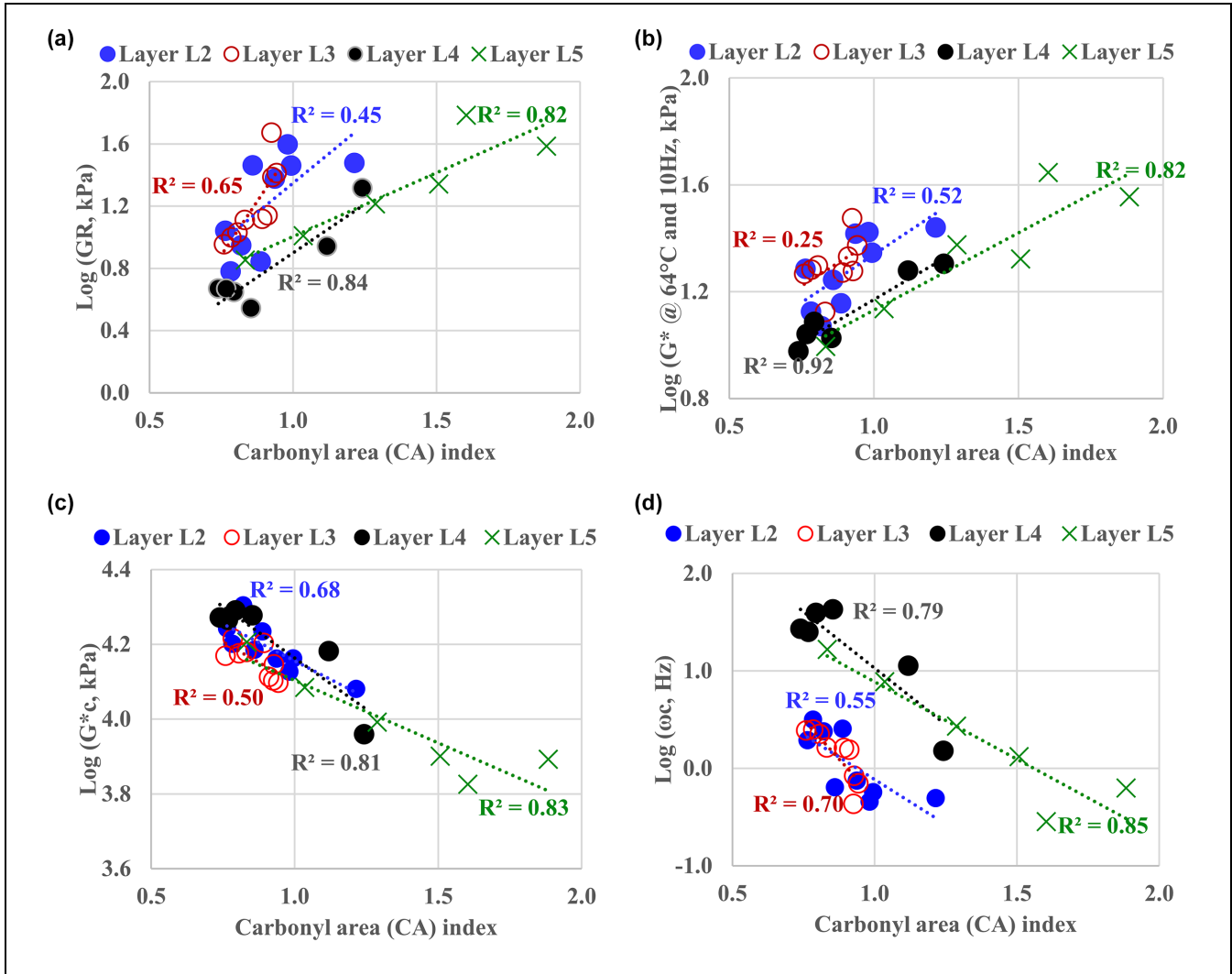


Figure 10. Correlations between the carbonyl area (CA) index and (a) log (Glover–Rowe [GR] parameter, kPa), (b) log (G^* at 10 Hz and 64°C, kPa), (c) log (G_c^* , kPa), and (d) log (ω_c , Hz).

extracted from the L4 layer were found to show much flatter curves compared to the other layers. However, the same base binder (PG 64-16) was used for all intermediate layers, as shown in Table 1. This might be attributed to the quality of RAP used in the L4 layer. For all intermediate layers, 25% RAP by weight of the total mix was used. Several other researchers have also reported that the properties of RAP play an important role in controlling the performance of asphalt mixes (7, 33, 34). Also, the binder extracted from sub-lift L4-2 at year 4 showed a slightly greater stress–strain curve area compared to samples taken in other years of the L4-2 sub-lift. As discussed earlier, the L4-2 sub-lift at year 4 has a relatively higher percent air voids (6.6%) and binder content (5.9%) compared to samples taken in other years (Figure 6). This may be attributed to slightly greater aging, which results in better fatigue performance. Several other

researchers also reported that slight aging improves the fatigue performance of asphalt binder (21, 29, 35). Also, the shear-stress curve for L2-1 was found to have a slightly higher shear strength and stiffer post-peak slope compared to other sub-lifts at year 7. A relatively higher air void content is expected to cause severe aging effects for the L2-1 sub-lift sampled in year 7.

Figures 12 and 13 illustrate the fatigue performance parameters calculated for extracted binders from intermediate AC layers (L2–L4) for different pavement sampling years. Figures 12a, 12b, and 13a show the fatigue lives calculated from binder LAS testing at 2.5%, 5%, and 10% strain levels, respectively. Figure 13b shows the variations of the new binder fatigue performance parameter ($\Delta|G^*|_{peak \tau}$) proposed by García Mainieri et al. (21). A similar trend was observed for fatigue lives (N_f) at different strain levels and $\Delta|G^*|_{peak \tau}$ parameters.

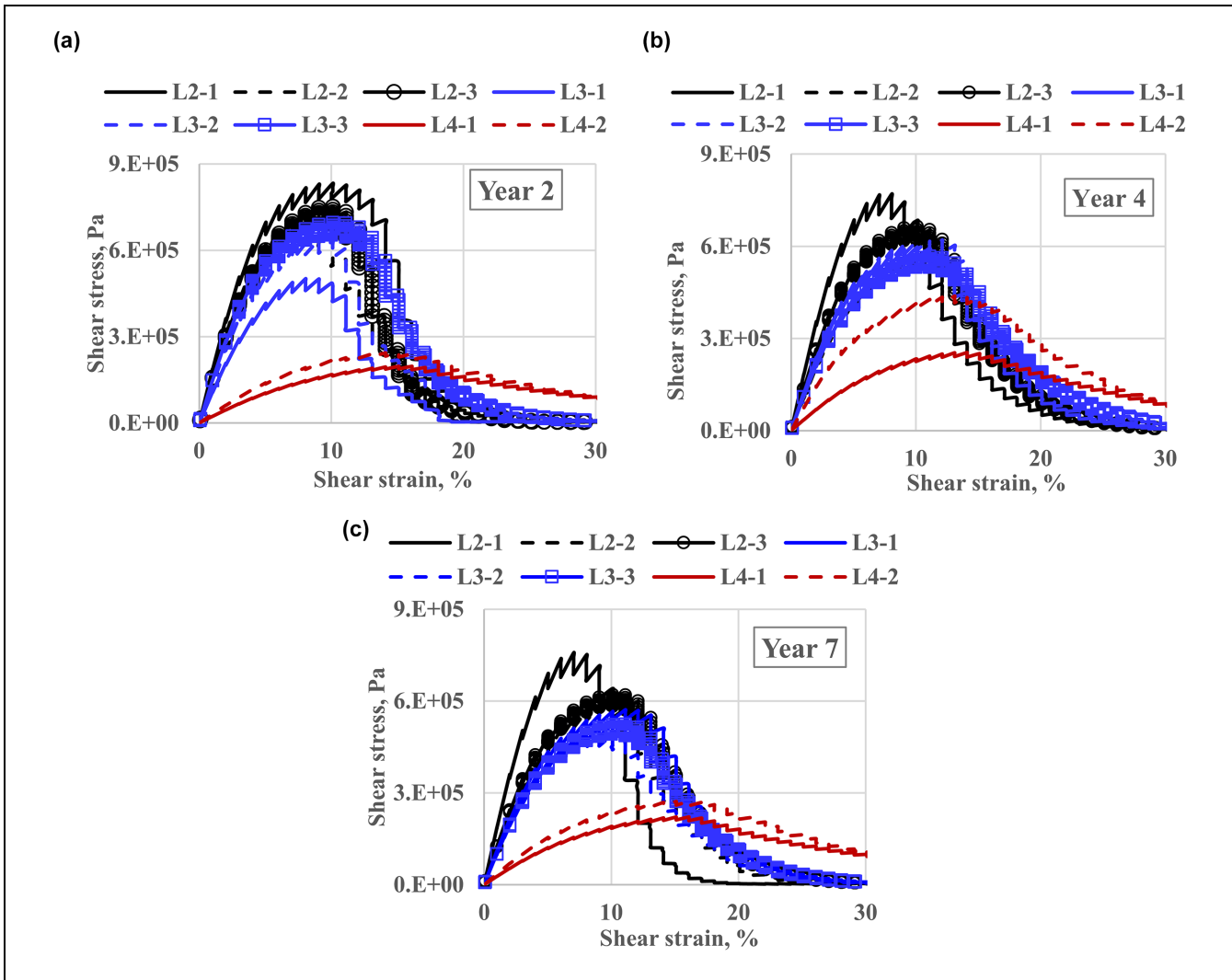


Figure 11. Shear-stress versus shear-strain curves for extracted binders at (a) year 2, (b) year 4, and (c) year 7.

Higher fatigue lives at all strain levels were observed for the L4-2 sub-lift at year 4 compared to all the other years. At 10% strain level, fatigue lives found for years 2, 4, and 7 using the AASHTO 391-20 calculation method for L4-2 sub-lift were 6.32×10^3 , 2.79×10^4 , and 8.83×10^3 , respectively. The values of $\Delta|G^*|_{peak \tau}$ at 2, 4, and 7 years of service lives for the L4-2 sub-lift were 45.2%, 55.9%, and 50.9%, respectively. Therefore, both fatigue life (N_f) and $\Delta|G^*|_{peak \tau}$ reflect similar information with respect to the binder fatigue performance. A slightly higher degree of aging for the L4-2 sub-lift at year 4 is expected to cause this higher fatigue performance. Other researchers have also reported improvement in binder fatigue performance up to a moderate level of aging and then a decrease in fatigue performance after more extreme aging (21, 29, 35).

The L3-2 sub-lift at year 7 was found to show lower binder fatigue performance compared to all other years. At the 10% strain level, fatigue lives found for years 2, 4, and 7 for the L3-2 sub-lift were 3.58×10^4 , 2.73×10^4 , and 1.32×10^4 , respectively. The values of $\Delta|G^*|_{peak \tau}$ observed after 2, 4, and 7 years in the field for the L3-2 sub-lift were 48.7%, 46.1%, and 41.2%, respectively. As shown in Figures 6 and 7, the L3-2 sub-lift at year 7 has far fewer air voids and lower aging indices. It can also be seen that the binder fatigue performance was lower at year 7 compared to other years (years 2 and 4) for sub-lifts L3-2, likely because of the better compaction and consequent reduced aging. Better fatigue performance of asphalt mixes with improved compaction has been reported by other researchers and is well known (36, 37). The effect of better compaction for the intermediate AC

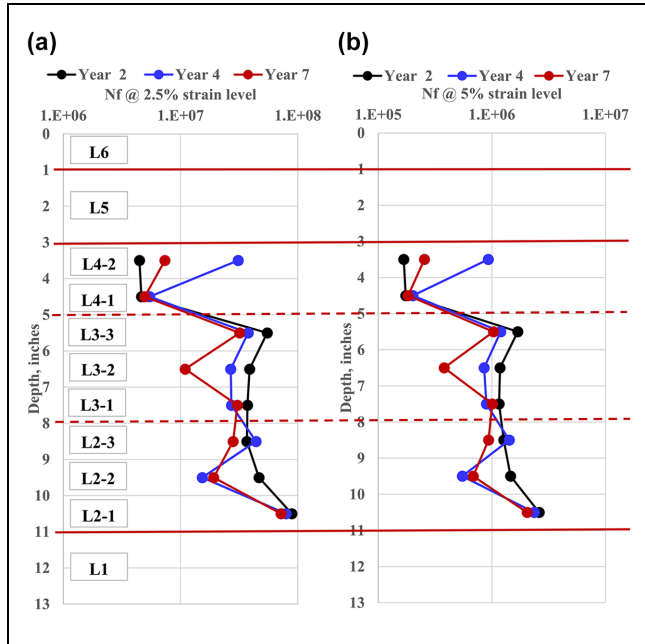


Figure 12. Fatigue life of extracted binders for intermediate asphalt concrete layers from linear amplitude sweep testing at (a) 2.5% and (b) 5% strain levels.

layer may not be explained properly using the binder fatigue life (N_f) and $\Delta|G^*|_{peak \tau}$ parameter.

Effect of Long-Term Laboratory Aging

As discussed earlier, the L3-2, L3-3, and L3-1 sub-lifts collected at year 4 were further aged in the laboratory for 5, 13, and 20 days at 85°C. Similar field aging indices were observed before this additional aging for these sub-lifts, as shown in Figures 6 and 7. The CA index values found at year 4 for sub-lifts L3-1, L3-2, and L3-3 were 0.89, 0.83, and 0.91, respectively. Therefore, these sub-lifts were considered to have the same initial aging condition before further long-term laboratory aging protocols.

Figure 14 presents the correlations between the CA index and different rheological aging indices before and after the long-term laboratory aging. Strong correlations were observed between the CA index and rheological parameters after considering long-term laboratory aging. The correlation increased as expected any time there was a statistical relationship between the variables and the data range increases for them. For example, the R^2 value increases from 0.25 to 0.95 for the CA index and logarithm of G^* @ 64°C and 10 Hz after the additional data from extended laboratory aging are added to the previously narrow range of those two variables because of a lack of aging in the field samples. The R^2 value increases from 0.70 to 0.98 for the CA index and logarithm of ω_C

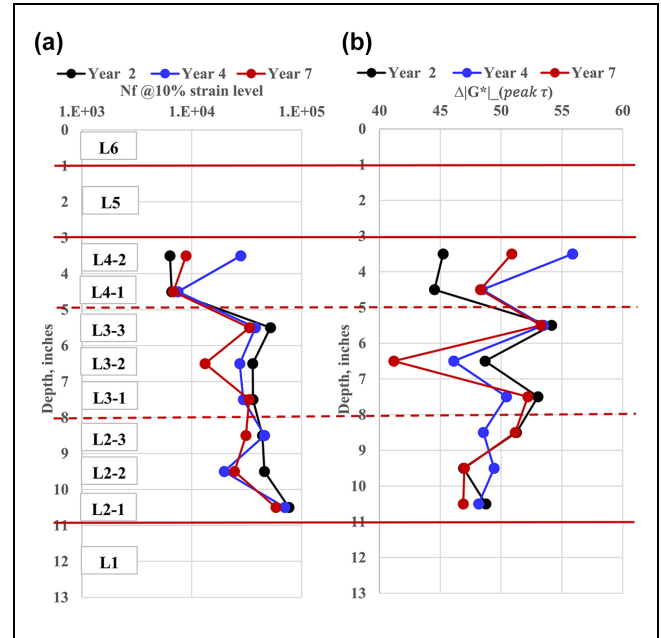


Figure 13. (a) Fatigue life of extracted binders for intermediate asphalt concrete layers at 10% strain levels and (b) $\Delta|G^*|_{peak \tau}$ parameter from linear amplitude sweep testing.

for the same reason. The scale for correlation assessment was 0–1 for all cases. The correlations after inclusion of the additional data for a wider range of aging indicate that the CA index can serve as a good chemical indicator in tracking the rheological changes in asphalt binders caused by aging. Several other researchers have reported similar findings (7, 11).

Figure 15 shows the change in binder fatigue lives from LAS testing with applied strain (Wöhler curve) for extracted binders collected before and after extensive laboratory aging. The slope of the Wöhler curves increases after laboratory aging for all cases, as shown in Figure 15. Similar findings were also reported by other researchers (22, 38). However, the laboratory aging up to 5 days at 85°C was found to improve fatigue lives. The binder fatigue lives observed at 10% strain level before and after aging (5 days at 85°C) were 2.73×10^4 and 8.29×10^4 cycles, respectively. Therefore, about three times longer fatigue lives were observed after laboratory aging of 5 days at 85°C at a 10% strain level. However, the laboratory aging at 13 and 20 days was found to reduce the fatigue lives at all strain levels. The binder fatigue lives observed at 10% strain level before and after 20 days of aging at 85°C were 2.95×10^4 and 5.83×10^3 cycles, respectively. Therefore, about five times shorter fatigue lives were observed after 20 days of laboratory aging at 85°C. Several other researchers have also reported a reduction in fatigue life after extreme aging (21, 29).

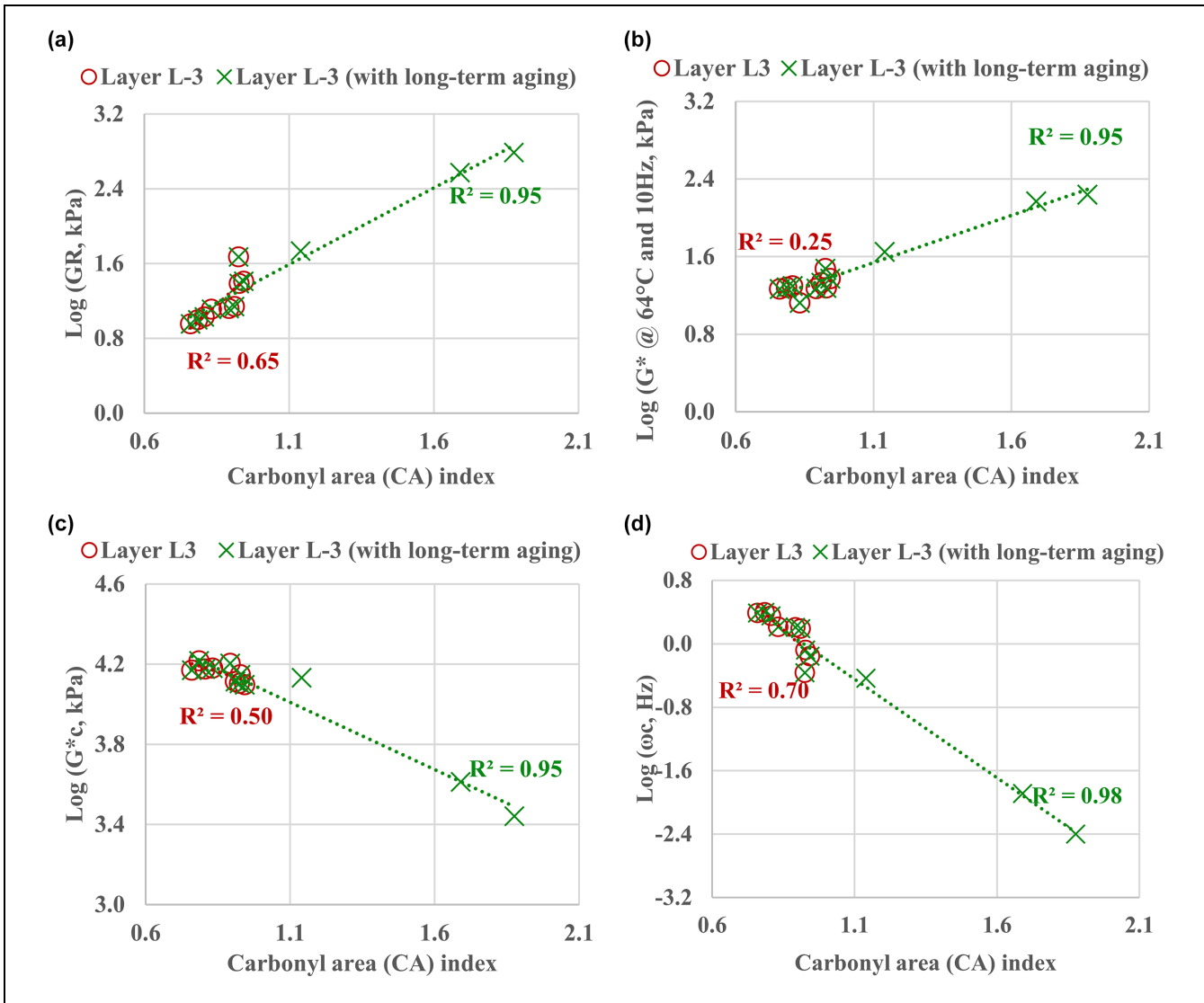


Figure 14. Correlations between the chemical property (CA index) and (a) log (Glover–Rowe [GR] parameter, kPa), (b) log (G^* at 10 Hz and 64°C, kPa), (c) log (G^*_c , kPa), and (d) log (ω_c , Hz) for layer L3.

Figure 16 shows the change in $\Delta|G^*|_{peak \tau}$ values after extensive laboratory aging. A similar trend was observed for $\Delta|G^*|_{peak \tau}$ values compared to the Wöhler curve. The $\Delta|G^*|_{peak \tau}$ parameter was found to increase after 5 days of laboratory aging at 85°C. The $\Delta|G^*|_{peak \tau}$ values found before and after 5 days of aging were 46.1% and 55.3%, respectively. However, 13 and 20 days of laboratory aging were found to reduce the $\Delta|G^*|_{peak \tau}$ values. The $\Delta|G^*|_{peak \tau}$ values observed before and after 20 days of aging were 50.4% and 39.1%, respectively. The binder extracted after 13 days showed a slightly lower $\Delta|G^*|_{peak \tau}$ value (37.8%) compared to the binder extracted after 20 days at 85°C (39.1%). However, both values were within one standard deviation, as shown in Figure 16. García Mainieri et al. (21) also reported a drop of $\Delta|G^*|_{peak \tau}$ values after long-term aging of asphalt binder.

Therefore, extensive aging is expected to reduce the fatigue performance of asphalt binders. Asphalt layers at intermediate depths are not expected to go through this extreme aging process where the influence of UV rays is not relevant, temperatures do not get as hot, and there is less access to oxygen. Improved compaction also plays a crucial role in safeguarding AC layers from an extreme aging environment by restricting the oxygen availability.

Conclusions

To date, most aging studies have focused on the aging of the asphalt surface layer. However, with the introduction of long-life asphalt pavements, it is important to study the effect of aging asphalt layers below the surface layer, termed “intermediate” AC layers in the pavements

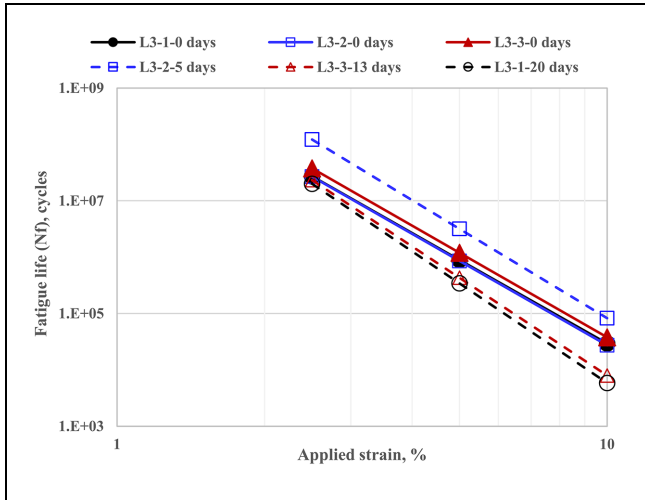


Figure 15. Wohler curve for layer L3 at year 4 before and after extensive laboratory aging.

described in this paper, which also contain up to 25% RAP. The top 1 in. (25 mm) of the pavement sampled consisted of an open-graded rubberized mix that was not evaluated in this study. In this study, binders were extracted from intermediate layers of asphalt pavement at different field ages (2, 4, and 7 years) and tested to evaluate the aging indices and fatigue performance. The

long-life pavement considered in this study was located in a hot climate region. The maximum daily temperature found for a representative weather station in the same climate region was always greater than freezing and had a maximum daily air temperature of 109°F (43.3°C) during the 7 years after construction. The following conclusions can be made based on this study.

- The increase in aging indices with an increase in service life is mostly observed in the top 4 in. (100 mm), primarily because of the impact of high temperatures at the surface. The availability of oxygen because of depth and the compaction (percent air voids) of each layer and the layers above it and binder contents were found to govern the aging of asphalt in the intermediate AC layers. The aging indices of the slabs collected after 7 years were slightly lower compared to the aging indices of the slabs collected at year 4 in the intermediate AC layers. This might be attributed to improved compaction for slabs collected in year 7. The variability of the material (RAP types and slight differences in silo time) might also have caused this variation. However, greater aging indices were observed for year 7 slabs compared to year 4 in the top 4 in. (100 mm).

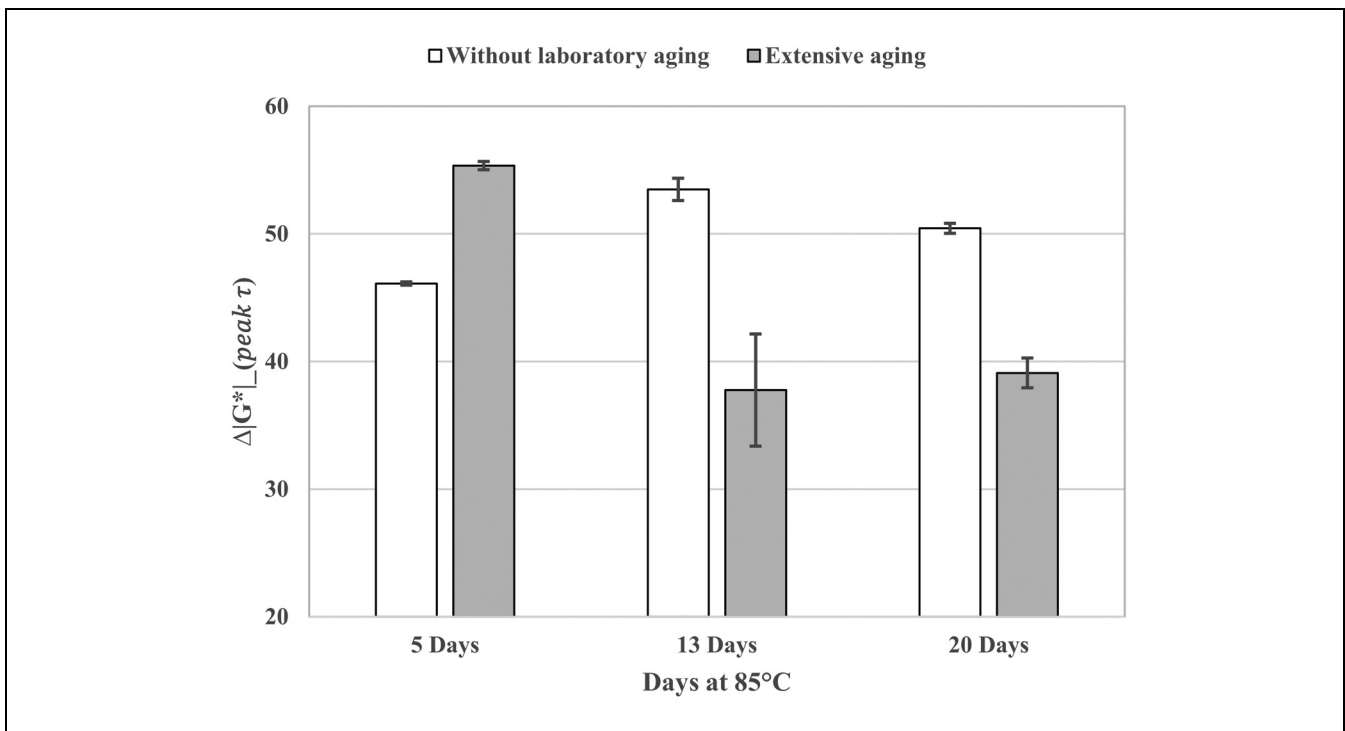


Figure 16. Change in $\Delta|G^*|_{peak \tau}$ values before and after extensive laboratory aging. Note: Error bars indicate one standard deviation of results.

- Good correlations were observed between the chemical property (CA index) and the rheological parameters for the AC layers above 4 in. (100 mm). R^2 values of 0.79–0.92 were observed between the CA index and other rheological indices for the PM surface layer and the intermediate layer to a depth of 4 in. There was no variability of aging or chemical indices, because of a lack of aging, below that depth.
- The properties of the RAP partially control the fatigue performance of asphalt mixes with higher RAP contents. The top of the intermediate layer was found to show different stress–strain curves compared to the intermediate layer material sampled from greater depths. This trend was observed even for samples collected at year 2 with no indication of aging for the top intermediate layer. However, a similar base binder was used for all three intermediate AC layers. The use of 25% RAP for all intermediate layers might result in this variation.
- The fatigue lives calculated by the LAS test (AASHTO T391-20) and $\Delta|G^*|_{peak} \tau$ parameter showed a similar trend in characterizing the extracted binders' fatigue performance. Binder fatigue performance was found to improve up to a moderate level of aging and then decrease with more extreme aging conditions. The benefits of better compaction cannot be explained using these methods.
- The sensitivity analysis conducted in this study indicates that the CA index can be used in tracking the rheological change of asphalt binders with aging. The fatigue lives at all strain levels and $\Delta|G^*|_{peak} \tau$ parameters were found to decrease after extensive laboratory aging. However, the extensive aging considered in this study may not be seen in the field for intermediate AC layers because of better compaction resulting in less access to oxygen, lower temperatures, and no UV rays at the depths of those layers.

In this study, field slabs up to 7 years old were considered. In the future, slabs will be collected at longer ages to continue to grow the understanding of the aging and binder fatigue performance of intermediate AC layers. Also, the pavement structure considered in this study has a rubberized open-graded AC layer. This open-graded top lift may result in more accessibility of oxygen for the underlying layers. In future studies, a long-life pavement structure with a dense-graded top AC layer will be considered to evaluate the effect of aging in the intermediate AC layers.

Acknowledgments

The authors would like to thank Irwin Guada, Julian Brotschi, and Anai Cazares-Ramirez from the University of California Pavement Research Center (UCPRC) for their constant support during this research.

Author Contributions

The authors confirm contribution to the paper as follows: study conception and design: M. Rahman, J. Harvey, D. Jones, R. Shrestha; data collection: M. Rahman, L. Jiao; analysis and interpretation of results: M. Rahman, J. Harvey, L. Jiao, R. Shrestha, D. Jones; draft manuscript preparation: M. Rahman, J. Harvey, L. Jiao, R. Shrestha, D. Jones. All authors reviewed the results and approved the final version of the manuscript.

Declaration of Conflicting Interests


The author(s) declared no potential conflicts of interest with respect to the research, authorship, and/or publication of this article.


Funding


The author(s) disclosed receipt of the following financial support for the research, authorship, and/or publication of this article: This paper describes research activities that were requested and sponsored by the California Department of Transportation (Caltrans).

ORCID iDs

Mohammad A. Rahman  <https://orcid.org/0000-0001-7855-5346>

John T. Harvey  <https://orcid.org/0000-0002-8924-6212>

Liya Jiao  <https://orcid.org/0000-0003-0648-693X>

David J. Jones  <https://orcid.org/0000-0002-2938-076X>

Data Accessibility Statement

The data used in this study will be made available on request.

References

1. Santero, N. J., J. Harvey, and A. Horvath. Environmental Policy for Long-Life Pavements. *Transportation Research Part D: Transport and Environment*, Vol. 16, No. 2, 2011, pp. 129–136.
2. Lee, E.-B., C. Kim, and J. T. Harvey. Selection of Pavement for Highway Rehabilitation Based on Life-Cycle Cost Analysis: Validation of California Interstate 710 Project, Phase 1. *Transportation Research Record: Journal of the Transportation Research Board*, 2011. 2227: 23–32.
3. Signore, J., B.-W. Tsai, and C. L. Monismith. *Development of Hot Mix Asphalt Pavement Performance Properties for Long-Life Pavement Design: Caltrans District 2, Interstate 5, Red Bluff, California*. UCPRC-TM-2014-03. University

- of California Pavement Research Center, CA, 2016, pp. 1–60.
4. Harvey, J., C. Monismith, R. Horonjeff, M. Bejarano, B. Tsai, and V. Kannekanti. Long-Life AC Pavements: A Discussion of Design and Construction Criteria Based on California Experience. International Symposium on Design and Construction of Long Lasting Asphalt Pavements, 2004, Auburn, Alabama, USA, 2004.
 5. Mandapaka, V. L., I. Basheer, and K. Sahasi. *Mechanistic-Empirical Design of a Long Life Flexible Pavement in Northern California, USA. Proc., 1st Conference of Transportation Research Group*, Bangalore, India, 2011.
 6. Rahman, M. A., R. Ghabchi, M. Zaman, and S. A. Ali. Rutting and Moisture-Induced Damage Potential of Foamed Warm Mix Asphalt (WMA) Containing RAP. *Innovative Infrastructure Solutions*, Vol. 6, No. 3, 2021, pp. 1–11.
 7. Harvey, J., J. Buscheck, J. Brotschi, M. Rahman, A. Mateos, and D. Jones. RAP and RAS in HMA Pilot Project on ELD 49: Material Testing, Observations, and Findings. UCPRC-TM-2022-04. University of California Pavement Research Center, CA, 2023, pp. 1–104.
 8. Rahman, M. A., M. Zaman, S. A. Ali, R. Ghabchi, and S. Ghos. Evaluation of Mix Design Volumetrics and Cracking Potential of Foamed Warm Mix Asphalt (WMA) Containing Reclaimed Asphalt Pavement (RAP). *International Journal of Pavement Engineering*, Vol. 23, No. 10, 2021, pp. 3454–3466.
 9. Rahman, M., J. Harvey, J. Buscheck, J. Brotschi, A. Mateos, D. Jones, and S. Pourtahmasb. Laboratory Performance and Construction Challenges for Plant Produced Asphalt Mixes Containing RAP and RAS. *Construction and Building Materials*, Vol. 403, 2023, p. 133082.
 10. Rahman, M. A., A. Arshadi, R. Ghabchi, S. A. Ali, and M. Zaman. Evaluation of Rutting and Cracking Resistance of Foamed Warm Mix Asphalt Containing RAP. Civil Infrastructures Confronting Severe Weathers and Climate Changes Conference, 2018, Springer.
 11. Rahman, M. A., J. T. Harvey, M. Elkashef, L. Jiao, and D. Jones. Characterizing the Aging and Performance of Asphalt Binder Blends Containing Recycled Materials. *Advances in Civil Engineering Materials*, Vol. 12, No. 1, 2023, pp. 1–17.
 12. Glover, C. J., R. Han, X. Jin, N. Prapaitrakul, Y. Cui, A. Rose, and A. E. Martin. *Evaluation of Binder Aging and its Influence in Aging of Hot Mix Asphalt Concrete: Technical Report*. Texas Department of Transportation, Research and Technology Implementation Office, Austin, Texas, 2014.
 13. Kim, Y. R., C. Castorena, M. D. Elwardany, F. Y. Rad, S. Underwood, A. Gundha, P. Gudipudi, M. J. Farrar, and R. R. Glaser. *Long-Term Aging of Asphalt Mixtures for Performance Testing and Prediction*. Transportation Research Board, The National Academies Press, Washington, D.C., 2018, pp. 1–124.
 14. Jin, X., R. Han, Y. Cui, and C. J. Glover. Fast-Rate-Constant-Rate Oxidation Kinetics Model for Asphalt Binders. *Industrial & Engineering Chemistry Research*, Vol. 50, No. 23, 2011, pp. 13373–13379.
 15. Oort, W. V. Durability of Asphalt-It's Aging in the Dark. *Industrial & Engineering Chemistry*, Vol. 48, No. 7, 1956, pp. 1196–1201.
 16. Liu, M., K. Lunsford, R. Davison, C. Glover, and J. Bullin. The Kinetics of Carbonyl Formation in Asphalt. *AIChE Journal*, Vol. 42, No. 4, 1996, pp. 1069–1076.
 17. Petersen, J. C. A Review of the Fundamentals of Asphalt Oxidation: Chemical, Physicochemical, Physical Property, and Durability Relationships. *Transportation Research Circular*, Vol. E-C140, 2009, pp. 1–78.
 18. Lau, C., K. Lunsford, C. Glover, R. Davison, and J. Bullin. *Reaction Rates and Hardening Susceptibilities as Determined From Pressure Oxygen Vessel Aging of Asphalts*. Transportation Research Record, Washington, D.C., 1992.
 19. He, Y., Z. Alavi, J. Harvey, and D. Jones. Evaluating Diffusion and Aging Mechanisms in Blending of New and Age-Hardened Binders During Mixing and Paving. *Transportation Research Record: Journal of the Transportation Research Board*, 2016. 2574: 64–73.
 20. Cao, W., and C. Wang. A New Comprehensive Analysis Framework for Fatigue Characterization of Asphalt Binder Using the Linear Amplitude Sweep Test. *Construction and Building Materials*, Vol. 171, 2018, pp. 1–12.
 21. García Mainieri, J. J., P. Singhvi, H. Ozer, B. K. Sharma, and I. L. Al-Qadi. Fatigue Tolerance of Aged Asphalt Binders Modified With Softeners. *Transportation Research Record: Journal of the Transportation Research Board*, 2021. 2675: 1229–1244.
 22. Chen, H., and H. U. Bahia. Modelling Effects of Aging on Asphalt Binder Fatigue Using Complex Modulus and the LAS Test. *International Journal of Fatigue*, Vol. 146, 2021, p. 106150.
 23. Christensen, D. W., and N. Tran. *Relationships Between the Fatigue Properties of Asphalt Binders and the Fatigue Performance of Asphalt Mixtures*. Transportation Research Record, Washington, D.C., 2021.
 24. Rahman, M. A., J. T. Harvey, and M. Elkashef. Update of the PG Binder Map in California Using the Enhanced Integrated Climate Model (EICM) and LTTBind Online. In *Proc., Airfield and Highway Pavements Conference*, 2023, pp.429–441.
 25. Liang, Y., R. Wu, J. T. Harvey, D. Jones, and M. Z. Alavi. Investigation Into the Oxidative Aging of Asphalt Binders. *Transportation Research Record: Journal of the Transportation Research Board*, 2019. 2673: 368–378.
 26. Hofko, B., M. Z. Alavi, H. Grothe, D. Jones, and J. Harvey. Repeatability and Sensitivity of FTIR ATR Spectral Analysis Methods for Bituminous Binders. *Materials and Structures*, Vol. 50, No. 3, 2017, pp. 1–15.
 27. Lamontagne, J., P. Dumas, V. Mouillet, and J. Kister. Comparison by Fourier Transform Infrared (FTIR) Spectroscopy of Different Ageing Techniques: Application to Road Bitumens. *Fuel*, Vol. 80, No. 4, 2001, pp. 483–488.
 28. Rowe, G. Prepared Discussion for the AAPT Paper by Anderson et al.: Evaluation of the Relationship Between Asphalt Binder Properties and Non-Load Related Cracking. *Journal of the Association of Asphalt Paving Technologists*, Vol. 80, 2011, pp. 649–662.

29. Singhvi, P., J. J. G. Mainieri, H. Ozer, B. K. Sharma, I. L. Al-Qadi, and K. L. Morse. Impacts of Field and Laboratory Long-Term Aging on Asphalt Binders. *Transportation Research Record: Journal of the Transportation Research Board*, 2022. 2676: 336–353.
30. Kose, S., M. Guler, H. U. Bahia, and E. Masad. Distribution of Strains Within Hot-Mix Asphalt Binders: Applying Imaging and Finite-Element Techniques. *Transportation Research Record: Journal of the Transportation Research Board*, 2000. 1728: 21–27.
31. Bell, C. A. *Summary Report on Aging of Asphalt-Aggregate Systems: Strategic Highway Research Program*. SHRP -A/IR-89-004. National Research Council, Washington, D.C., 1989.
32. Bell, C. A., A. J. Wieder, and M. J. Fellin. *Laboratory Aging of Asphalt-Aggregate Mixtures: Field Validation*. SHRP -A-90. National Research Council, Washington, D.C., 1994.
33. Dinis-Almeida, M., J. Castro-Gomes, and M. de Lurdes Antunes. Mix Design Considerations for Warm Mix Recycled Asphalt With Bitumen Emulsion. *Construction and Building Materials*, Vol. 28, No. 1, 2012, pp. 687–693.
34. Al-Qadi, I. L., H. Ozer, J. Lambros, A. El Khatib, P. Singhvi, T. Khan, J. Rivera-Perez, and B. Doll. *Testing Protocols to Ensure Performance of High Asphalt Binder Replacement Mixes Using RAP and RAS*. Report No. 0197-9191. Illinois Center for Transportation/Illinois Department of Transportation, 2015.
35. Jiao, L., M. Elkashef, J. T. Harvey, M. A. Rahman, and D. Jones. Investigation of Fatigue Performance of Asphalt Mixtures and FAM Mixes With High Recycled Asphalt Material Contents. *Construction and Building Materials*, Vol. 314, 2022, p. 125607.
36. Harvey, J. T., and B.-W. Tsai. Effects of Asphalt Content and Air Void Content on Mix Fatigue and Stiffness. *Transportation Research Record: Journal of the Transportation Research Board*, 1996. 1543: 38–45.
37. Harvey, J. T., J. A. Deacon, B.-W. Tsai, and C. L. Monismith. *Fatigue Performance of Asphalt Concrete Mixes and Its Relationship to Asphalt Concrete Pavement Performance in California*. UCPRC-RTA-65W485. University of California Pavement Research Center, CA, 1995.
38. Cao, X., H. Wang, X. Cao, W. Sun, H. Zhu, and B. Tang. Investigation of Rheological and Chemical Properties Asphalt Binder Rejuvenated With Waste Vegetable Oil. *Construction and Building Materials*, Vol. 180, 2018, pp. 455–463.

The contents of this paper reflect the views of the authors. They do not necessarily reflect the official views or policies of the State of California or the Federal Highway Administration.